Title
WIDE BAND DATA TRANSMISSION SYSTEM USING OPTICAL FIBERS

Authors
Leskovar, B.
Nakamura, M.
Turko, B.T.

Publication Date
1987-04-01

Lawrence Berkeley Laboratory
UNIVERSITY OF CALIFORNIA

Engineering Division

Presented at the IEEE 1987 Nuclear Science Symposium,
San Francisco, CA, October 21–23, 1987, and to
be published in the Proceedings

Wide Band Data Transmission System Using Optical Fibers

B. Leskovar, M. Nakamura, and B.T. Turko

April 1987

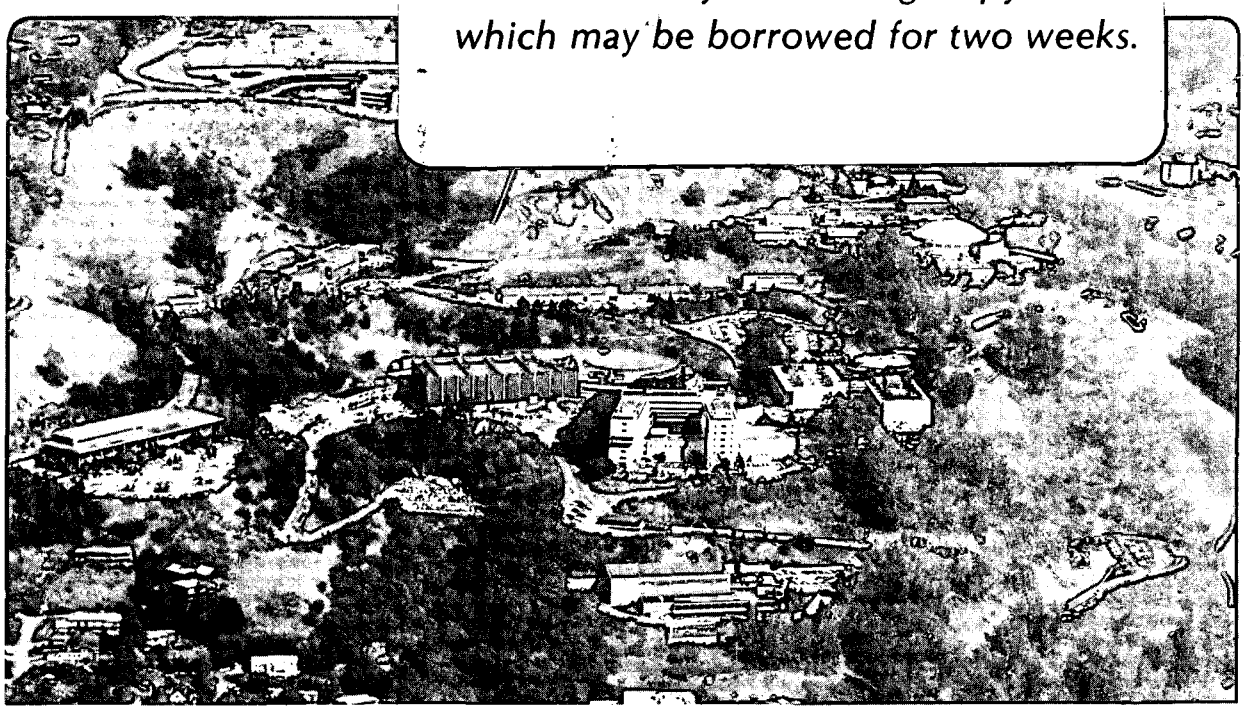

Prepared for the U.S. Department of Energy under Contract DE-AC03-76SF00098

DISCLAIMER

WIDE BAND DATA TRANSMISSION SYSTEM USING OPTICAL FIBERS

B. Leskovar, M. Nakamura and B.T. Turko

Lawrence Berkeley Laboratory
University of California
Berkeley, California 94720 U.S.A.

ABSTRACT

An ultra high speed data transmission system using optical fibers and gallium arsenide digital integrated circuits has been investigated. The system is designed to meet the increased data rate requirements of modern information processing systems as well as those of future imaging devices and high spatial resolution detectors. A description of the system which uses available components made for the transmission and reception of data at 780 Mbit/s rates is given. Methods for digitizing, multiplexing, demultiplexing, error checking, etc. are also described, and a discussion of the reliability of components is presented.

INTRODUCTION

The concept of guided lightwave communication along optical fibers has stimulated a major new technology over the past two decades. This technology profoundly impacts telephone and instrumentation systems as well as computer interconnections and system architecture. Fiber optic links provide several major advantages over conventional electronic communication systems. These include immunity to electromagnetic interference, and low transmission losses for very high data rates. It also makes possible thinner and lighter cables and has a strong potential for tens-of-kilometer-long repeaterless link capabilities extending to the gigahertz region.

The emergence of optical communication using fibers was made possible by the parallel development of low loss fibers, heterojunction lasers, light-emitting diodes (which emit in spectral regions of low fiber loss), and sensitive photon detectors. The technology of optical fiber communication systems is advancing at a very rapid rate. As the short optical wavelength multimode fiber systems are being field-proven and used commercially, the technology is progressing towards single-mode fiber systems in the long-wavelength region. For example, significant advances have been made in the fabrication of low-loss and low-dispersion optical fibers.[1] Losses of only 0.27 dB/km at 1.3 μm have been achieved for single mode fibers with minimum dispersion wavelengths near 1.3 μm. Furthermore, the development of optical sources, and optical receivers,for long wavelength applications is also advancing rapidly. Several experimental transmission systems capable of operating at a 4 Gbit/s rate over a distance of 103 km, and 2 Gbit/s over 170 km have been reported.[2-3]

Although these impressive results were obtained under highly optimized experimental conditions they do give an indication of future capabilities. It should be pointed out that at the present time practical high data rate optical transmission system are operating between 90 Mbit/s and 565 Mbit/s.[4]

In addition to the requirements placed on the optoelectronic components of these systems, considerable attention was paid to the associated logic circuit families with switching speeds in the microwave region. Such capability is necessary for multiplexing and demultiplexing functions. These functions have been implemented using both silicon and gallium arsenide (GaAs) technology.[5,6] Devices based on GaAs technology have become available recently for applications in practical systems with a data rate capability of 1.5 Gbit/s.[6]

Although the major thrust for development of high data rate fiber optic systems has been for long distance communication links, the local data communication needs have given a new impetus for the development of advanced system components. The recent systems for local communication, such as computer interconnections, rf distributions in phased array radars and instrumentation for basic and applied research, require a high data rate capability. Specifically, instrumentation systems, using wide amplitude dynamic range and high spatial resolution charge-coupled device image sensors[7] together with image intensifiers,[8] with frames rates of 500 frames/s or higher, require extraordinary high data rate transfer capability.

Studies of existing fiber optics digital transmission systems and future requirements for transmitting data from high spatial resolution charge coupled imaging devices (CCD) have indicated that there is a great need to develop a next generation of wide band systems.

At present, data from CCD imaging arrays are transmitted over single fiber optic cables in serial fashion at 180 MHz rates. Such fiber optic cable system is capable of transmitting data at a rate of maximum 300 MHz[9]. There is also the requirement that these data be transmitted in the matter of a few milliseconds. 180 MHz data rates are adequate for the present imaging systems with CCD image sensors (up to 256 x 256 pixels) whose analog signals are digitized to 8 bits. However, the next generation of imaging systems will have larger CCD image sensors (512 x 512 pixels) and the analog signals will be digitized with up to 12 bit resolution. This puts significantly greater demands on the bit rate capability of the data transmission system.

We have investigated the feasibility of designing and developing a high speed data transmission system to meet the demands of these higher data rates using presently available components and materials. Data from a CCD camera will be digitized and transmitted to receivers over a distance of several tens-of-kilometers. The data will then be error checked, processed and placed into memory storage. The data transmitting, receiving, demultiplexing, etc. will be done within a time frame of a few milliseconds.

SYSTEM CONSIDERATIONS

A number of semiconductor area imaging sensors that are available today offer high spatial resolution and large signal dynamic range suitable for this application. However, most of them are designed for standard 30 frames/second video rates while the

required single frame readout time of a few milliseconds would need a sensor driven at a few hundred frames/second. Each frame is composed of a mosaic of square picture elements (pixels), organized in rows and columns. In this case, the mosaic has 512 rows and 512 columns, i.e. the frame consists of 262,144 pixels.

Transfer of charge, generated by the individual pixels, is done by driving the device clocks in proper pulse sequences. One video line at a time is shifted by vertical clocks and then moved past a charge sensitive amplifier by horizontal clocks. The charge from each pixel, entering the amplifier, produces a proportional voltage signal at the amplifier output. Great charge transfer efficiency of such devices allows a signal to noise recovery ratio close to 10000: 1 under certain conditions. Unfortunately, most of these devices can not be clocked fast enough to allow a few milliseconds frame readout through a single charge sensing port.

The problem can be solved by splitting the sensor area into smaller sections, each having an individual charge sensitive amplifier but sharing the same transfer clocks. For instance, a 512 x 512 pixel sensor can be divided first across the center in two equal sections and then each section again divided into six blocks of 86 x 256 pixels. Such division would allow placing the charge sensitive amplifier of each section close to the edge of the sensor, making easier the extraction of individual video signals, as shown in Fig. 1.

Each block would now have only 22016 pixels, allowing a few milliseconds signal frame readout with clock rates not exceeding 15 MHz. The penalty paid is that the external circuits needed for the analog and digital image frame processing are also increased by a factor of 12. This is the same as having 12 cameras operating at the same time instead of one.

Processing of individual video signals should be carefully designed in order to preserve the inherently high signal to noise ratio. Each video line consists of 256 discrete pulses, having amplitudes proportional to the integrated illumination charge of the correspon ding pixel area (14 μm x 14 μm). Typical interfering artifacts are caused by the clock transient feedthrough pulses superimposed upon the video signal. Also it is extremely important to minimize crosstalk interference between image sections which could cause double exposure effects on the image and reduce the image quality.

In order to achieve the bit rates necessary to meet the time frame requirement, the data transmission system would require fiber optics for data transmission and gallium arsenide (GaAs) devices (capable of Gbit/s speeds) for handling and processing data in critical high data rate areas. Standard bipolar silicon technology can be used in places where speeds are non-critical. The data is to be stored in a memory with a battery backup system. The memory, in turn, will be accessible to a computer for analysis and to an image processor for immediate real-time display of the memory data.

A simplified diagram of the system is shown in Figure 2. After the image is temporarily stored in the CCD image sensor, the analog information in each image sensor block will be read out at a 15 MHz rate and digitized by flash analog to digital converters (ADC's) with 12-bit resolution. Pixels from all twelve blocks of the CCD image sensor will be read out simultaneously and digitized by twelve ADC's after which a parity bit is added to form a 13 bit word. By time division multiplexing four blocks of the CCD image sensor onto a single fiber optic data transmission line, the multiplexed data of all twelve blocks can be transmitted on three fiber optic lines each at a data transmission rate of 780 Mbit/s (15 MHz x 13 bits x 4).

For multiplexing the 12 blocks onto fiber optic cables, we had options of selecting 12 blocks onto 1 fiber optic cable, 6 onto 2, 4 onto 3 or 3 blocks onto 4. The 4 blocks onto 3 fiber optic cables option gives a more conservative 780 Mbit/s rate whereas the 6 onto 2 option would have given a 1.17 Gbit/s rate which would push the limits of the present GaAs devices and printed circuit board technology. While the 6 onto 2 multiplexing scheme would have been desirable from the standpoint of using less fiber optic cables and associated components, the more conservative data rates of the chosen system should produce more overall reliability. Using these data transmission rates and multiplexing all twelve blocks onto three fiber optic lines, all the data will be transmitted, received and processed within a few milliseconds.

A row sync word (RSW) and two Dummy Words comprise the first four words to be transmitted at the beginning of each group of four rows from four blocks. The RSW is made of two redundant words to guard against accidental coincidence of two data words having identical bit patterns. As an added precaution the RSW and Dummy Words have even parity while the data words from the CCD image sensors have odd parity. Two Dummy Words are added to RSW to make demultiplexing simpler by being compatible with the 4 blocks-to-one fiber optic cable format, and in addition they could be used for row identification. The multiplexed data will modulate transmitting laser diodes which will be coupled onto fiber optic cables.

Transmission of data using non-return to zero (NRZ) digital coding format is proposed in order to maintain the best possible bit error rate (BER) because bandwidth requirements are effectively one-half that of a return to zero (RZ) pulse code format. Other pulse code formats such as bi-phase, amplitude modulation, frequency modulation and phase modulation have been rejected as being more complex or requiring more bandwith than NRZ. At present, most performance characterizations for high speed optical communication components and systems are normalized to NRZ code standards. Descriptions of transmission and reception of data will be made on the basis of NRZ techniques.

The receiver signals are sent to a clock recovery and phase-locked loop system where the receiver clock is synchronized with the data received. Row sync word (RSW) detection circuits synchronize the incoming data with each group of 1024 words which corresponds to a group of four rows from the four multiplexed blocks from the CCD image sensor. Demultiplexing the incoming data is accomplished by a serial-to-parallel conversion of the serial bit stream. Once the data are stored in the parallel data register, parity checks are made on the incoming data. Error flags are raised if parity or row synchronization should fail.

Data from the parallel data register are transferred to memory in parallel fashion, but the row sync and dummy words are not put into memory. One possible alternative is to have the Dummy Words con-

tain row count information for absolute row synchronization.

High Data Rate Digitizer and Multiplexer

A description of the operation of the time division multiplexing scheme shown in Fig. 3, follows. By applying the CLK A signal at the appropriate time, the RSW and Dummy Words will be transmitted just prior to the transmission of real data and will become the first data words for a row. The 13 bit words formed by the 12 bit flash ADC and parity bit are the real data which are temporarily stored in Buffer Registers I, II, III and IV (not shown). The clocks, CLK B and CLK C, serve to both parallel load real data into the shift registers (S/R's) and serially shift data out of the S/R's when appropriately timed with their respective parallel/serial (PAR/SER) control signals. Control Gates I, II, III and IV are also applied in a timely manner to present the real data to the shift registers for parallel loading. At the right side of the diagram, all data signals are applied to the "D" input and the D-flip flop at some predetermined time via the signals A, B, C and D which control their respective gates. The parallel-to-serial action provides the time division multiplexing function for the data.

The Idle Data gated by the D control signal are composed of a series of one-zero-one-zero bits and are sent prior to the sending of any data to provide a pre-signal to the receiver. This signal allows the receiver clock recovery circuit and phase-locked loop an alternating bit pattern with sufficient transition states to readily synchronize the receiver clock to the incoming data. This ensures that when data of any consequence is sent, the receiver system is already synchronized for the data. The Idle Data are sent any time there is a known gap in the bit serial stream, such as during horizontal or vertical blanking. In this manner, the receiver clock will always be correctly synchronized.

The Reclock signal serves to transmit the data with a constant phase relationship with the highly stable transmitter clock for all data. Variations in transit times on the printed circuit board can easily cause phase shifts for the different data, which, if transmitted without reclocking, would be detrimental to the operation of the receiver clock synchronization. By reclocking the D-flip flop with the data as shown, the data are formatted in the NRZ data format code as they are sent to the laser diode for transmission over the fiber optic cables. Gallium arsenide (GaAs) devices are used throughout in Fig. 3.

Optical Source for Wide Band Transmission System

Semiconductor lasers are the most frequently employed as light sources in optical broadband systems because of their compactness and high level of efficiency in comparison to other sources. The semiconductor compounds, indium gallium arsenide phosphide $In_{1-x}Ga_xAs_yP_{1-y}$ has emission wavelengths between 0.92 and 1.62 μm, depending on the composition, making it particularly suitable for 1.3 μm zero dispersion wavelength of an optical silica fiber.

Various types of semiconductor lasers, their structure and characteristics as well as pertinent optical processes, such as absorption, spontaneous emission and stimulated emission are extensively treated in the literature.[10-11] For the wide band data transmission system of particular interest are laser structures that employ a variation in the real-refractive index along the junction plane to form an optical waveguide. These index-guided injection InGaAsP lasers are free from the light output nonlinearities because of excellent mode stability. The index-guided laser with a thermoelectric cooler, temperature sensor unit power monitor and associated circuitry are packaged in a single module. A block diagram of such a laser light source is shown in Fig. 4. The integral thermoelectric cooler maintains the laser and power monitoring photodiode temperatures at 25°C over an ambient temperature range of -40°C to + 65°C. Also, an internal InGaAsP PIN photodiode, mounted directly behind the laser diode functions as a power detector. The photodiode monitors the emission from the rear facet of the laser and controls the optical power level sent into the fiber.

Based on the above given considerations and using available components the optical source for wide band transmission system should be an index-guided injection InGaAsP laser with the following characteristics: emission wavelength = 1.3 μm, maximum data rate capability = 1.7 Gbit/s, CW optical power = 2.5 mW (+4dBm), rise and fall time smaller than 100 ps, RMS spectral width smaller than 3 nm, laser threshold current = 20 mA, laser forward current for maximum optical output =40 mA, laser forward voltage at output power of 1 mW = 1.3 V, and life greater than 10^5 hours.

Transmission Characteristics of Optical Fibers

The basic transmission mechanisms of the various types of optical fiber waveguide have been discussed elsewhere[12-14]. Basically, the most important transmission of optical fiber characteristics are attenuation and bandwidth.

The attenuation or transmission loss, of optical fibers is influenced by the material composition, the fiber preparation technique and the waveguide structure. In particular, the attenuation is determined by material optical absorption, material scattering, macrobending and microbending losses, mode coupling radiation losses and losses due to leaky modes. Furthermore, there are also losses at the input and output connectors. In Figs. 5 and 6 the typical attenuation spectrum is shown for some state-of-the-art multimode and single-mode optical fibers.[12-14] The attenuation characteristics are shown for three major fiber preparation processes: (a) inside vapor deposition, (b) vapor-phase axial deposition and (c) outside vapor deposition.

In practical optical fibers prepared by above mentioned processes a major cause of signal attenuation below a wavelength of about 1.5 μm is Rayleigh scattering.

Rayleigh scattering results from excitation of small irregularities on the order of λ/10 in the medium by the propagating electromagnetic wave. It is strongly wavelength dependent. The attenuation coefficient per unit length L_S can be expressed as $L_S = A/\lambda^4$, where A is a constant which depends on the refractive index of the medium, the average photoelastic coefficient, the isothermal compressibility and the temperature at which the glass can reach a state of thermal equilibrium and is closely related to the annealing temperature. This λ^{-4} dependence results in considerable attenuation at shorter wavelengths.

In addition to the Rayleigh scattering, attenuation in optical fiber can be caused by Mie scat-

tering from large defects and by Brillouin scattering from the thermally driven density fluctuations that are present in fibers at room temperature. Furthermore, at high power levels, nonlinear loss mechanism such as stimulated Raman and Brillouin scattering can further increase the attenuation and limit the dynamic range of the fiber. Another major extrinsic loss mechanism in fibers is caused by absorption of light in negative hydroxyl ions (OH) trapped during fiber processing. This produces sharp absorption peaks at 1.25 and 1.39 μm and smaller peaks at 0.75 and 0.97 μm. Since these peaks are present to some degrees in even the highest quality fiber, transmission at these wavelength is usually avoided. In Fig. 6 the ultraviolet absorption loss is also shown. This loss is due to the stimulation of electron transition within the silica glass by higher energy excitations. Its value was estimated by extrapolating the data from GeO_2-doped silica glass. Furthermore, in Fig. 6 the infrared absorption loss is shown. This loss was obtained by extrapolation from the loss characteristics of GeO_2-doped silica-core fiber and optical data for pure glass at long wavelengths where strong absorption bands are caused from the interaction of photons with molecular vibrations within the glass.

It appears from Figs. 5 and 6 that three major manufacturing processes are giving approximately the same attenuation level for both multimode and single-mode fibers. The single-mode attenuation level is intrinsically slightly lower than multimode one because of lower core dopant concentrations. In both figures the typical attenuation highest level is also shown indicating tolerances of the fiber manufacturing process.

The information carrying capacity or bandwidth of a fiber is inversely related to its total dispersion. The total dispersion consists of mode, material and waveguide dispersions. Mode dispersion is dependent only on the fiber, while the material and waveguide dispersions depend on the width of the wavelength spectrum from the light source.

Mode dispersion occurs in multimode fibers because different modes travel different effective distances through the fiber. This causes light pulse to spread out temporarily as it travels along the fiber. For multimode step-index fiber this effect seriously limits the band-width to approximately 20 MHz per kilometer of length, or 20 MHz x km. For multimode graded-index fibers the bandwidth is increased to approximately 1 GHz x km.

The rms pulse broading due to the modal dispersion for a graded index fiber is given by[12-14]:

$$t_m = \frac{Ln_1\Delta^2}{20(3c)^{1/2}} \qquad (1)$$

Where L is the length of the fiber, n_1 is the refractive index of the fiber core, Δ is the relative refractive index difference defined for $\Delta \ll 1$ as $\Delta = (n_1-n_2)/n_1^2$, n_2 is the refractive index of the fiber cladding and c is the velocity of light in the vacuum. Typically, for $L = 10^3$ m, $n_1 = 1.5$, $\Delta = 0.01$ and $c = 2.998 \times 10^8$, the rms pulse broadening is 14.4 ps/km for ideal fibers.

Material dispersion is caused by the variation in refractive index of glass with wavelength. This leads to the light pulse spreading even when different wavelengths follow the same path, because the speed of light in the fiber equals the speed of light in a vacuum scaled by the index of refraction at a given wavelength. The rms pulse broadening due to the material dispersion is given by:

$$t_c \simeq \frac{t_h L}{c}\left|\lambda \frac{d^2 n_1}{d\lambda^2}\right| \qquad (2)$$

Where t_h is the spectral width of the light source, L is the fiber length, c is the velocity of light in vacuum, λ is the wavelength, and n_1 is the refractive index of the fiber core.

Also the pulse broadening can be expressed in terms of material dispersion parameter

$$M = \frac{\lambda}{c}\left|\frac{d^2 n_1}{d\lambda^2}\right| \quad [\text{ps/km x nm}] \qquad (3)$$

$$\text{as} \quad t_c \simeq t_h L M \qquad (4)$$

Typically, for multimode graded index fiber having $m \simeq 100$ ps/km x nm and a light emitting diode used as a light source with an rms spectral width of 20 nm at wavelength of 1.3 μm, the rms pulse broadening is 2 ns/km. However, if an injection laser is used as a light source with an rms spectral width of 1 nm at the same wavelength, the the theoretical rms pulse broadening is approximately 100 ps/km for the optimum value of the core refractive index profile. Because of variations of the refractive index profile with optical wavelength and over the lengths of the fiber, the practical pulse broadening values lie in the range 200-500 ps/km.

Waveguide dispersion, which is also wavelength dependent, is significantly smaller than the material dispersion in multimode fibers because light is almost completely confined to the core.

Multimode dispersion in a data transmission system can be completely avoided using a single-mode fiber which carries light only in a single-wavelength mode. In such a fiber no dispersion between modes can exist and very large bandwidths are possible. However, material and waveguide dispersions limit the bandwidth of single-mode fiber. Waveguide dispersion occurs because light in single-mode fiber is not confined completely to the core. About 20% of the light travels in the cladding adjacent to a step-index core. The refractive index of the cladding is lower than that of core and so the light travels somewhat faster than in core. The wavelength dispersion is wavelength-dependent, although the change in wavelength dispersion with wavelength is smaller than that of material dispersion. Furthermore, the material and waveguide dispersion can have different signs and thus completely cancel each other out. In conventional germanium-doped silica fibers this "zero-dispersion" wavelength is near 1.3 μm.

In Fig. 7 the material dispersion of silica, curve (a), and the waveguide dispersion of step-index fibers having core diameters d of 3.5 and 11 μm are presented as a function of the wavelength, curve (b) and (c). The combined effect of material and waveguide dispersion is also shown, curves (d) and (e). Reducing the core diameter has two effects. The zero dispersion point is shifted to longer wavelengths and the gradient of the dispersion in the vicinity of zero gradient point is reduced.

The zero dispersion point can be also shifted over a range of wavelengths by controlling Ge-doping density.

The material and waveguide rms pulse broadening for a fiber of length L is given by the following equation[14]:

$$t_s = \frac{t_h\, 2\pi L}{c\lambda^2} \frac{d^2\beta}{dp^2} \qquad (5)$$

Where t_h is the light source rms spectral linewidth centered at a wavelength λ, c is the velocity of light in vacuum, p is the propagation constant for the mode in a vacuum, and β is the propagation constant for a mode within the fiber core of refractive index n_1. The constant β varies nonlinearly with the wavelength and it can be expressed in terms of the relative refractive index difference Δ and the normalized propagation constant b as:

$$\beta = pn_1[1-2\Delta(1-b)]^{1/2} \qquad (6)$$

When equations (5) and (6) are combined the dependence of the pulse broadening on the fiber material's properties and normalized propagation constant b can be obtained. These calculations give rise to three interrelated effects which involve cross-product terms. The final dispersion can be separated in three composite dispersion components in such a way that one of the effects dominate each term. These dominating effects are: 1) the material dispersion parameter defined by $\lambda/c\ d^2n/d\lambda^2$, where $n = n_1$ or n_2 for the core and cladding, respectively; 2) the wave-guide dispersion parameter defined as $Vd^2(bV)/dV^2$, where V is the normalized frequency of the fiber defined by $V = 2\pi\ n_1\ (2\Delta)^{1/2}d/\lambda$, (d is the fiber core radius); 3) a profile dispersion parameter which is proportional to $d\Delta/d\lambda$.

In addition to the dispersion components considered above for a single-mode fiber, there are other higher order effects which impose limitation on the maximum bandwidth. These together with secondary effects, such as birefringence which arises from ellipticity or mechanical stress in the fiber core, give a fundamental lower limit to pulse spreading between 3.5 and 5 ps/km x nm. The maximum theoretical bit rate for optical channel can be estimated from the expression $B_T\ (max) = 0.2/t_s$ (bit/s). In this case the maximum bit rate is between 40 and 57 Gbit/s if an injection laser with rms spectral linewidth of t_h = 1 nm is used as a pulsed light source and there is a small amount of intersymbol interference in the channel. Consequently, the maximum theoretical bandwidth length product, B x L, is between 40 GHz x km and 57 GHz x km.

Based on the above and available components the data transmission link will have the following specifications: transmission wavelength = 1.3 μm, transmission data rate = 780 Mbit/s, single mode optical fiber core diameter = 8.3 μm, fiber outside diameter = 125 μm, optical fiber attenuation = 0.4 dB/km, maximum dispersion of optical fiber = 3.2 ps/km, and strength = 50 kpsi.

The Optical Receiver

Optical receiver designs for fiber transmission have been addressed in various papers. Most of these papers have dealt with receivers for telecommunication applications. In this section results of the analysis from Ref. 14-15 will be presented for digital systems, emphasizing the trade-offs between conflicting receiver design requirements for operation at bit rates above 700 Mbit/s.

As a receiver bandwidth is increased to accommodate higher transmission bit rates its sensitivity decreases. The receiver sensitivity is defined as the minimum optical power level required at the receiver input which allows it to operate reliably with a bit error rate less than a desired value. In this case it is given as the average optical power $\bar{P}$ required for a bit error rate, (BER), of 10^{-9}.

Bit error rate is defined by the ratio of bits incorrectly identified to the total number of bits transmitted. The receiver sensitivity is also often specified in terms of the average optical power $\eta\bar{P}$ which is detected by the photodetector, where η is the quantum efficiency of the photodetector. Until recently, PIN photodiodes fabricated from InGaAsP alloys grown epitaxially on high quality InP substrates were regarded, as most suitable for use in the low-noise optical receivers of long wavelength communication systems. However, recently, to increase sensitivity at high bit rates, extensive research has been done on detectors with internal gain. Of these devices reverse biased, avalanche photodiodes (APDs), exhibit high-speed response in the absence of large dark currents.

Depending on their configuration, preamplifiers for optical receiver are classified into two types: high impedance and transimpedance designs, Fig. 8. The high impedance preamplifiers offer the lowest noise level and hence the highest detection sensitivity. However, the frequency response is limited by the RC time constant at the input making necessary an equalizer following the preamplifier to extend the receiver bandwidth. Furthermore, this design has limited dynamic range due to the high-input load resistance. The transimpedance amplifiers have a large dynamic range and bandwidth due to their negative feedback. However, because of the thermal noise of the feedback resistor the preamplifier noise level is higher and sensitivity is lower than that of a high-impedance design.

Based on the above analysis and availability of the components the optical receiver design for the wide band transmission system will have the following characteristics: planar InGaAs PIN photodetector having responsivity of 0.65 A/W at wavelength = 1.30 μm, maximum data rate capability = 1.7 Gbit/s, transimpedance GaAs preamplifier sensitivity (at 1.7 Gbit/s (NRZ) and BER = 10^{-9}) = -21 dBm, preamplifier sensitivity at 880 Mbit/s = -27 dBm, maximum optical input power (NRZ) for BER = 10^{-9} and 1.7 Gbit/s = -7 dBm, transimpedance = 0.95 kΩ, high-frequency cutoff at -3 dB from midband = 1.1 GHz, and lifetime larger than 10^8 hours.

Data Processing and Storage

Figure 9 is a simplified diagram showing the clock recovery, demultiplexing, error checking and processing of data for memory. The receiver signals are sent to a clock recovery and phase-locked loop system where the receiver clock is synchronized with the data received. The row sync word (RSW) detection circuits synchronize the incoming data with each group of 1024 words which corresponds to a group of four rows from four multiplexed blocks from the CCD image sensor. Demultiplexing the incoming data is accomplished by a serial-to-parallel conversion of

the serial bit stream by taking the data from the Shift Register and temporarily storing it in the Parallel Data Register. Once the data are stored in the Parallel Data Register, parity checks are made on the incoming data. Row synchronization error detect circuits look for row sync errors and error flags are raised if parity or row synchronization should fail.

By handling the incoming data in groups of rows from each of the four blocks, by serial to parallel demultiplexing, the demands on memory speed will be reduced from 780 MHz to 15 MHz. This is a data rate easily met by memory chips using complementary metal oxide semiconductor (CMOS) technology. CMOS memory devices require very little power in the standby condition which is a desirable characteristic for backup battery operation.

Data from the image sensor are transferred to memory in parallel fashion, but the row sync and dummy words are ignored and not put into memory. The memory storage system can be made in a straight-forward way using memory mapping techniques to reconstruct the image for visual display. For critical viewing, data will be processed by a computer.

CONCLUSIONS

Using available digital IC's, electro-optical and opto-electrical transducers and fiber optic cable, the design and implementation of an optical wide band data transmission system for 780 Mbit/s can be accomplished. The transmission and reception of data over single mode fiber optic cables at 1300 nm wavelength will be realized with very low bit error rates (BER) of 10^{-9}.

The reliability of GaAs components is very high for thermal, radiation, leakage and electromigration effects. System reliability is determined by the use of error checking schemes such as parity and row synchronization checks. Good thermal management techniques and layout with constant impedance lines and low differential delay will ensure excellent high speed operation with reliability.

ACKNOWLEDGEMENTS

This work was performed as part of the program of the Electronics Research and Development Group of the Lawrence Berkeley Laboratory and the Diagnostics Development Group of the Lawrence Livermore National Laboratory. The work was supported by the U.S. Department of Energy under Contract Numbers DE-AC03-76SF00098 and W-7405-Eng-48. Reference to a company or product name does not imply approval or recommendation of the product by the University of California or the U.S. Department of Energy to the exclusion of others that may be suitable.

REFERENCES

1. V.A. Bhagavatula,G.E. Berkey and A. Sarkar, Scattering Loss in Single Mode Fibers by Outside Process, Tech. Dig. Sixth Topical Meeting Opt. Fiber Communication, paper MK2, pp. 22-25, March 1983.

2. A.H. Gnauck, B.L. Kasper, R.A. Linke, R.W. Dawson, T.L. Koch, T.J. Bridges, E.G. Buckhard, R.T. Yen, D.P. Wilt, J.C. Campbell, K. Ciemecki Nelson and L.G. Cohen, 4-Gbit/s Transmission over 103 km of Optical Fiber Using a Novel Electronic Multiplexer/Demultiplexer, J. Lightwave Technology, Vol. LT-3, pp. 1032-1035, October 1985.

3. A.H. Gnauck, R.A. Linke, B.L. Kasper, K.J. Pollock, K.C. Reichmann, R. Valenzuela, and R.C. Alferness, Coherent Lightwave Transmission at 2 GBit/s over 170 Km of Optical Fiber Using Phase Modulation, Technical Digest of Optical Fiber Communication/International Integrated Optics and Optical Fiber Communication Conference, pp. 270-273, Optical Society of America, 1987.

4. Y. Hayashi, Y. Kobayashi, and K. Aida, 445-Mbit/s Transmission Field Experiment at 1.55 μm Wavelength Region Over 80 km Using Under Sea Optical-Fiber Cable, J. of Lightwave Technology, Vol. LT-4, No. 7, pp. 942-947, July 1986.

5. N. Yosikai, S. Kawanishi, M. Suzuki, and S. Konaka, Monolithic Integrated 4:1 Multiplexer and Demultiplexer Operating up to 4.8 Gbit/s. Electronics Letters, Vol. 21, No. 4, pp. 149-150, February 1985.

6. J.H. Kemps, and R.M. Hicking, GaAs Digital ICs Impact Fiber System Design, Optoelektronik Magazin-European Laser-Opto Technology, Vol. 2, No. 2, pp. 501-504, 1986.

7. B.T. Turko, Fast Readout of CCD Images, IEEE Transactions on Nuclear Science, Vol. NS-32, No. 1, pp. 576-580, February 1985.

8. B. Leskovar, E.J. Jerbic, and G. Zizka, Performance Characteristics Studies of Image Intensifier Having Short Luminescence Decay Time, IEEE Transactions on Nuclear Science, Vol. NS-34, No. 1, pp. 453-457, February 1987.

9. "Fiber-Optics Data Transmission and Storage System Hardware Reference Manual,"EG&G Energy Measurement Report, EG&G 10282-4011, July 1986.

10. C.H. Henry, Spectral Properties of Semiconductor Lasers. Semiconductors and Semimetals, Vol 22, Part B, W.T. Tsang, Ed., pp. 153-204, Academic Press, 1985.

11. AT&T Technologies, 555 Union Blvd. Dept 50AL203140, Allenton, PA 18103.

12. J. Gowar, Optical Communication Systems, Prentice-Hall International, Inc., London 1984.

13. B.J. Ainslie, and C.R. Day, A Review of Single-Mode Fibers with Modified Dispersion Characteristics, Journal of Lightwave Technology, Vol. LT-4, No. 8, pp. 967-979, August 1986.

14. B. Leskovar, M. Nakamura,. and B. Turko, Optical Wide Band Data Transmission System, Lawrence Berkeley Laboratory Report, LBL-23113, March 15, 1987.

15. R.G. Smith and S.D. Personick, Receiver Design for Optical Fiber Communication Systems, Semiconductor Devices, Topics in Applied Optics, Vol. 39, H. Kressel, Ed., pp. 89-160, Springer Verlag, Heidelberg, 1982.

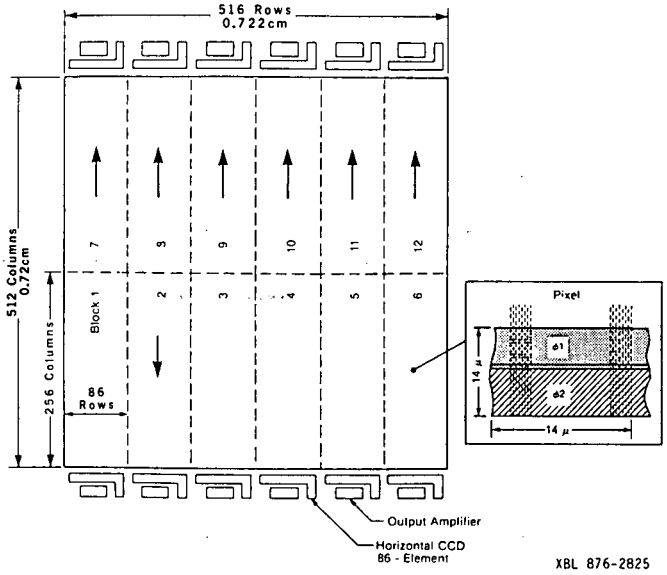

Figure 1. CCD sensor architecture.

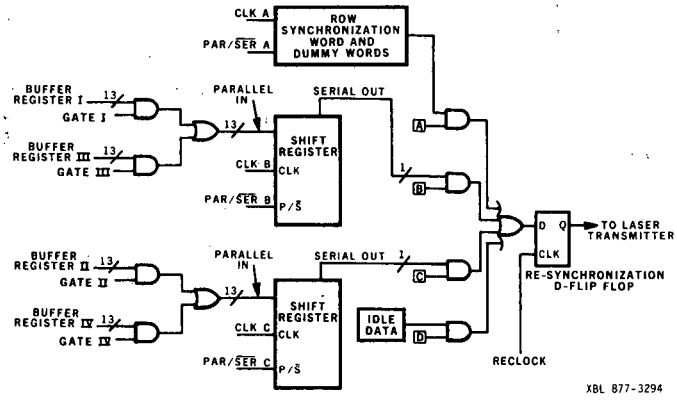

Figure 3. Time division multiplexing scheme - parallel to bit serial.

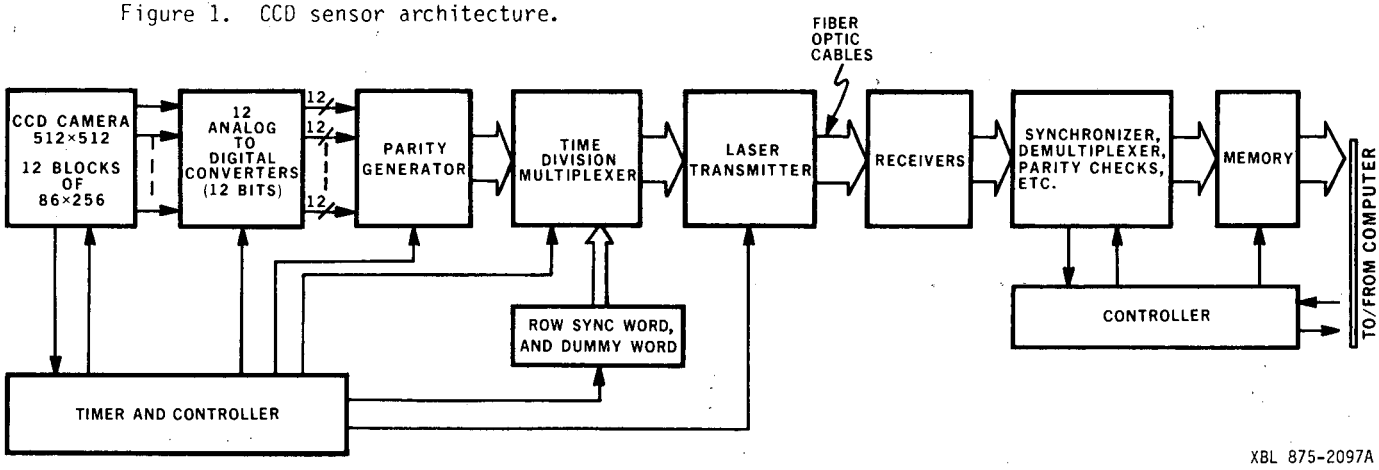

Figure 2. Simplified block diagram for optical wide band data transmission system.

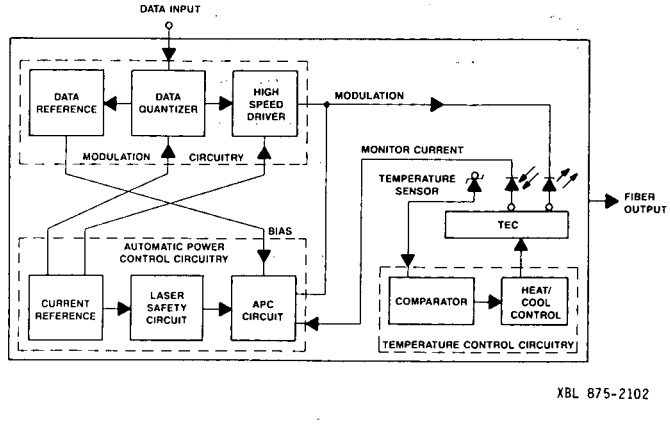

Figure 4. Index-Guided laser light source block diagram.

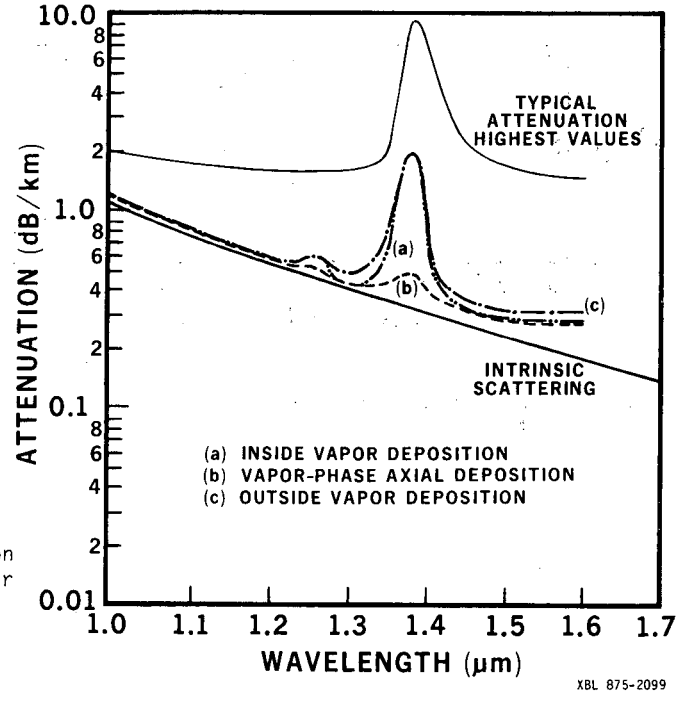

Figure 5. Attenuation as a function transmission wavelength for multimode optical fiber growth processes: (a) inside vapor deposition, (b) vapor-phase axial deposition, and (c) outside vapor deposition.

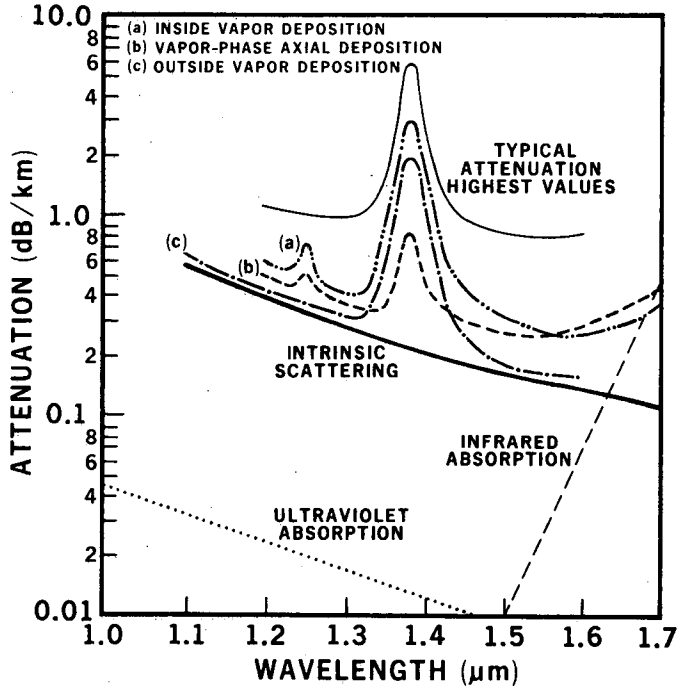

Figure 6. Attenuation as a function of transmission wavelength for single-mode optical fibers.

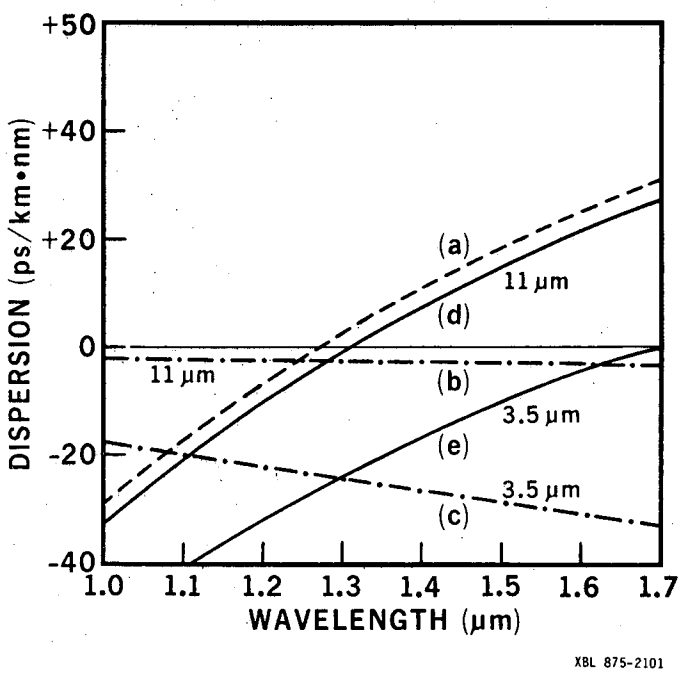

Figure 7. Dispersion curves of step-index single-mode fibers.

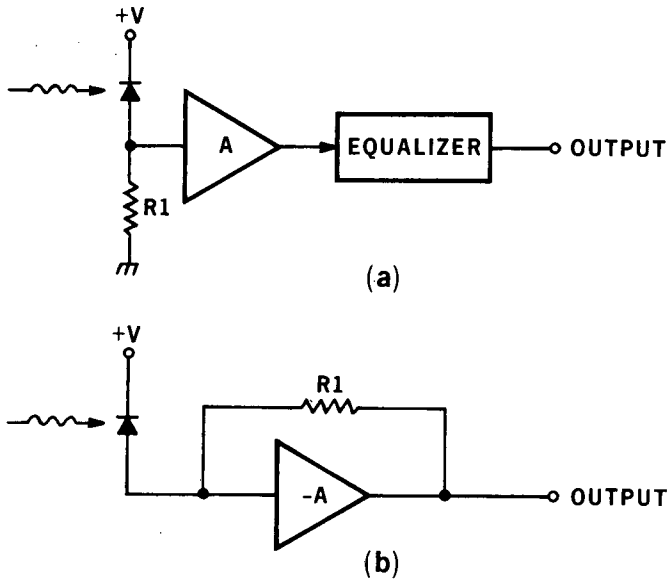

Figure 8. (a) High impedance and (b) transimpedance designs of optical receiver preamplifier.

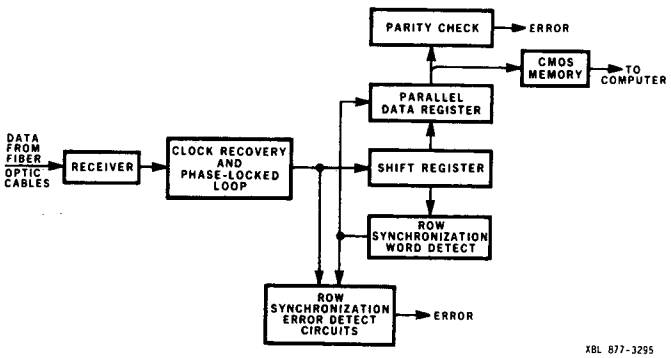

Figure 9. Diagram showing synchronization, demultipiexing, error checking and data preparation for memory.

LAWRENCE BERKELEY LABORATORY
TECHNICAL INFORMATION DEPARTMENT
UNIVERSITY OF CALIFORNIA
BERKELEY, CALIFORNIA 94720